Soft Matter

Cite this: DOI: 10.1039/c2sm25742d

www.rsc.org/softmatter

PAPER

Poly-ethylene glycol induced super-diffusivity in lipid bilayer membranes†

Thibault Tabarin,[a] Aaron Martin,[a] Robert J. Forster[ab] and Tia E. Keyes*[ab]

Received 30th March 2012, Accepted 2nd July 2012
DOI: 10.1039/c2sm25742d

Fluorescence lifetime correlation spectroscopy (FLCS) has been used to probe the influence of PEG-8000 on the fluidity of fluorescently labeled planar supported lipid bilayers on ozone plasma treated glass. The lipid membrane compositions examined were; DOPC, DOPC/DOPS (80/20 mol/mol) and DMPC, with and without cholesterol. The lateral diffusion coefficients (D) for supported lipid bilayer films of these layers without cholesterol were 7.9 ± 0.2, 7.9 ± 0.4 and 5.5 ± 0.1 $\mu m^2 s^{-1}$ respectively. The high fluidity reflected the super-hydrophilicity (contact angle of 0) of the ozone treated plasma glass substrate. Using DOPE conjugated Atto 655 as a probe, exposure of the lipid bilayer to a 30% wt/wt aqueous solution of PEG, followed by washing, dramatically increased the diffusion coefficients of the probe within the film. For example, the diffusion coefficient for the DOPC bilayer increases by nearly an order of magnitude to 51.4 ± 2.6 $\mu m^2 s^{-1}$. The autocorrelation curves for DOPC/DOPS (80/20 mol/mol) and DMPC bilayers required a two-component model for adequate fit of their behaviour yielding both fast and slow components of the diffusion. In all cases, when hydrophilic DOPE–Atto 655 was used as the probe, treatment of the lipid bilayer with PEG resulted in non-Brownian diffusion. Importantly, the observed diffusion behavior observed depends on the identity of probe. In contrast, when a hydrophobic probe (DOPE–NapthBodipy) was employed PEG showed relatively little impact on the observed diffusion rates. This was attributed to orientation of the reporter probe in the lipid bilayer and its aqueous interface. Specifically, DOPE–Atto 655 is believed to associate strongly with PEG mesh at the aqueous interface of the lipid bilayer, its diffusion strongly influenced by the structure in this region, whereas DOPE–NapthBodipy remains in the interior of the bilayer where it is relatively uninfluenced by PEG.

Introduction

The phospholipid bilayer is an omnipresent structure in the cell. Its key roles are to support the mobility and function of the transmembrane proteins, which constitute approximately 30% of all proteins in the human body[1] and to provide a semi-permeable barrier for regulation of ion exchange at the living cell.[2] For some time, the accepted model of cell membrane structure was the fluid mosaic membrane model where proteins were envisaged as embedded in a homogeneous sea of lipid.[3] More recently, the view on cell membranes has progressed to a more sophisticated model that includes heterogeneity in composition and compartmentalization. In this model discrete domains are distinguished which feature distinctive dynamic and structural properties.[4] In the living membrane the identity of phospholipid, lipid–lipid, lipid–protein and protein–protein affinity all influence membrane behavior. The dynamics of membrane diffusion in this less homogeneous two-dimensional picture does not conform to the ideal case of Brownian motion. A number of techniques have been applied to study organization and dynamics of planar membranes but the different parameters at different length scales of observation can lead to discrepancies in the results and interpretation.[4] For instance AFM gives precise topography at the nanometer scale,[5] electron spin resonance can provide useful ensemble measurements of lipid diffusion in vesicles in solution,[6] fluorescence recovery after photobleaching is suitable for investigating the diffusion on supported bilayer but the diffraction limit on spatial resolution renders it rather unhelpful in the observation of the effects of small domains and in the study of multiple groups of molecules diffusing with different rates.[1] To assess the mode of diffusion and determine the diffusion coefficient on planar supported lipid bilayers, fluorescence correlation spectroscopy (FCS) is the technique of choice.[7,8] It has proven particularly useful in the study of systems that exhibit anomalous diffusion that does not conform to well-defined free diffusion models.[9,10] FCS is therefore, valuable in tracking reorganization occurring at the nanometer scale, below the resolution limit.

The phospholipid membrane appears to be very sensitive to the nature of its surroundings. For instance, the addition of salts can induce reorganization of the membrane into small domains[11] or

[a]*National Biophotonics and Imaging Platform, National Center for Sensor Research, Dublin City University, Dublin 9, Ireland. E-mail: tia.keyes@dcu.ie*
[b]*School of Chemical Sciences, Dublin City University, Dublin 9, Ireland*
† Electronic supplementary information (ESI) available. See DOI: 10.1039/c2sm25742d

may alter the fluidity of the bilayer.[12] Deformation of the membrane structure induced by pressure exerted by a natural polymer mesh anchored to the membrane has also been reported.[13]

Various polymers have been used with biological and biomimetic samples. One of the most important biocompatible polymers to emerge is polyethylene glycol (PEG).[14] PEG has a strong influence on the phospholipid membrane, *e.g.*, it is known to alter membrane fusion in vesicles[15] and cells and to alter the permeability of the phospholipid membrane. Consequently medical applications are emerging which exploit the ability of PEG to mediate membrane fusion[16] and PEG is already widely applied in transmembrane transport, most notably for drug delivery.[17] PEG has been exploited as a hydrophilic cushion used to support planar lipid bilayers to reduce interactions of transmembrane proteins inserted into such membranes with the substrate.[18–20] It has also been used as a support to aid in the formation of the bilayer.[21] In spite of its wide application with membranes and cells, surprisingly few studies have been reported on the influence PEG has on the membrane structure/diffusion dynamics. Kuhl *et al.* described PEG as reducing the attraction between the lipid bilayer leaflets[22] and Lee *et al.* reported interesting insights into the structural interaction between PEG and lipid membrane.[6] However, to our knowledge there have been no reports on the influence of PEG on the fluidity or dynamics of the lipid bilayer or on the role the fluorescent reporter of diffusion plays in interrogating these dynamics. Such studies may yield insights into why PEG improves permeability of the membrane and on its ability to mediate membrane fusion.

In this contribution, using fluorescence lifetime correlation spectroscopy (FLCS), we show that the apparent dynamics of a planar supported lipid bilayer is strongly modified by its exposure to a solution of PEG 8000.[14,15] The diffusion of probe, DOPE–Atto655, increases by almost an order of magnitude when the layer is treated with PEG. A detailed examination of the parameters describing the diffusion behavior show that diffusive motion deviates from freely diffusing Brownian motion on exposure to PEG, and we observed super-diffusion[23] that is associated with fractal motion of the probe. The impact of changing the compositions of bilayer, the nature of the head group, and the charge, on the influence of the PEG on the membrane diffusion dynamics, are reported. The role of the hydrophilicity of the probe is discussed, wherein it was found that super-diffusion was only observed when a hydrophilic probe; DOPE–Atto 655 was used as reporter. When a hydrophobic probe (DOPE–NapthBodipy) was employed super-diffusion was not observed. This was attributed to partitioning of the hydrophilic reporter probe into the PEG film at the bilayer–water interface. A preliminary examination of the influence of cholesterol on the bilayer fluidity was undertaken. Cholesterol rich lipid mixtures also show varying responses to PEG and indicate that cholesterol, by changing the physical properties of the membrane, modifies the interaction between PEG and the bilayer.

Experimental

Chemicals and materials

The lipids used in this study; 1,2-dioleoyl-*sn*-glycero-3-phosphocholine (DOPC), 1,2-dimyristol-*sn*-glycero-3-phosphocholine (DMPC), 1,2-dioleoyl-*sn*-glycero-3-phospho-L-serine (DOPS) and cholesterol (Chol) were purchased from Avanti Polar Lipids (Delfzijl, Nederland). 1,2-dioleoyl-*sn*-glycero-3-phosphoethanolamine (DOPE) and all other chemicals including polyethylene 8000 MW (PEG) and Tris buffer were purchased from Sigma Aldrich (Wicklow, Ireland). The Atto-655 NHS ester was purchased from Atto-tech (Siegen, Germany) and the NapthBodipy was synthesized in house according to a reported procedure.[17]

NapthBODIPY-NHS

2,6-Diethyl-1,3,5,7-tetramethyl-8-[(2-fluorophenyl)-6-methoxy-1,5-naphthyridine-3-carboxylate]-4,4′-difluoroboradiazaindacene (100 mg, 0.16 mmol) and *N*-hydroxy succinimide (24 mg, 0.21 mmol) were dissolved in anhydrous MeCN (17 ml). Added to this was a solution of DCC (44 mg, 0.21 mmol) in anhydrous MeCN (5 ml), the reaction mixture was allowed to stir under N_2 until all the starting material had been consumed (TLC). The reaction mixture was then filtered and concentrated to dryness with the crude solid purified on silica gel (50 : 50 EtOAc : hex) which gave the *title compound* **12** (75 mg, 65%) as a bright red solid, R_f 0.6 (50 : 50 EtOAc : hex); (found: C, 65.5; H, 5.2; N, 10.1. $C_{37}H_{35}BF_3N_5O_4$ requires C, 65.2; H, 5.2; N, 10.3%); δ_H(400 MHz; $CDCl_3$) 9.40 (s, 1H, Naph *H*-2), 8.27 (d, $J = 9.2$ Hz, 1H, Naph *H*-7), 7.40 (pt, 1H, Ar *H*), 7.22 (d, $J = 8.8$ Hz, 1H, Naph *H*-8), 7.14 (d, $J = 8.0$ Hz, 1H, Ar *H*), 7.11 (d, $J = 9.6$ Hz, 1H, Ar *H*), 3.72 (s, 3H, OCH_3), 2.81 (bs, 4H, CH_2 NHS), 2.47 (s, 6H, $2 \times CH_3$), 2.27 (m, 4H, $2 \times CH_2$), 1.44 (s, 3H, CH_3), 1.32 (s, 3H, CH_3), and 0.93 (t, $J =$ 7.2 Hz, 6H, CH_3) ppm; ^{13}C NMR ($CDCl_3$) δ 167.6, 161.7, 159.9, 159.6, 158.2, 155.7, 153.6, 153.0, 146.4, 143.9, 142.9, 139.1, 138.4, 137.6, 137.2, 137.1, 136.9, 136.4, 132.0 (d, $J_{CF} = 18.8$ Hz), 131.4 (d, $J_{CF} = 2.5$ Hz), 129.6, 129.2, 122.7 (d, $J_{CF} = 2.3$ Hz), 122.1, 122.0, 120.5, 118.5, 114.6 (d, $J_{CF} = 18.7$ Hz), 62.7, 52.8, 24.6, 24.5, 16.1, 16.0, 13.6, 11.6, 11.5, 10.8, and 10.7 ppm. λ_{max} (ε [M^{-1} cm^{-1}]) = 527 nm (47 000 ± 1300); λ_{em} = 547 nm (λ_{ex} = 532 nm), Φ_f = 0.54 (±0.06), $\tau_f = 4.7$ ns.

Phospholipid labeling. The labeling of DOPE with Atto 655 and NaphthBodipy were carried out using amine reactive (NHS ester form) functionalized dyes. The NHS ester was conjugated to the amine present on the head group of DOPE, and purification of the resulting lipid was performed using chromatography on a silica gel column.[24] For both Atto-655 and for NaphthBodipy, TLC showed the disappearance of the starting material and a single product spot correlating to the dye labeled DOPE. R_f 0.3 (DCM/H_2O/MeOH 70 : 4 : 26).

Buffer and PEG 8000 solution. The buffer containing 20 mM of Tris and 100 mM of NaCl was filtered with 0.1 μm cellulose Whatman filter from Fischer Scientific (Dublin, Ireland). The PEG solution was made up as 30% wt in water. All the solutions were prepared with MilliQ water with a resistivity of 18.2 MΩ.

Lipid formation

The bilayer was formed using a vesicle adsorption technique adapted from the literature,[11,25,26] which leads to a defect free lipid bilayer with very high reproducibility. In brief, the lipids, dissolved in chloroform, were mixed at the appropriate mole

ratio in a glass vial; DOPC pure, DOPC/DOPS (80/20), DMPC pure, DOPC/Chol (60/40), DOPC/DOPS/Chol (48/12/40) with the dye at a mole ratio of 1/50 000 (labeled lipid/unlabeled lipids). Then the chloroform was gently evaporated under a nitrogen flow to form a multilayer of lipid on the vial surface. The vial was placed under vacuum for 2 hours to remove the remaining chloroform. After rehydration with Tris buffer and vortexing for 30 seconds, the solution was extruded above the transition temperature (at 22 ± 2 °C for DOPC and DOPC/DOPS mixture and with the cholesterol and at 25 °C for DMPC) using a polycarbonate membrane mini-extruder with 50 μm pore size from Polar Avanti Lipids (Instruchmeistry, Neederland). The average size of the vesicles was determined by DLS to be around 100 nm. The vesicle solution at 2.5 mg ml^{-1} (concentration of lipid) was then diluted 10 times in a solution containing the Tris buffer and 5 mM $CaCl_2$ to improve the lipid bilayer film formation and lead to a defect free bilayer.[27] In 90% of cases, the bilayer was perfectly uniform on areas larger than 0.1 mm^2, with no vesicle adsorption evident on the surface. The solution was injected into the cell chamber, which was heated at 25 °C. After 5 min of incubation, the cell chamber was rinsed with 3 ml of Tris buffer solution corresponding to 10 times the volume of the cell. The lipid film quality was assessed using fluorescence microscopy and FCS. The images obtained for the defect free bilayer display a homogeneous fluorescence. The presence of patches of different fluorescence intensity or bright spots easily identifies the presence of defects (ESI†). Over the time-scale of the experiments when the bilayer remained defect free and displays normal fluidity, no decrease of the fluorescence is observed even after several hours of acquisition. This means the reservoir of probe can be considered as infinite (there is no boundary condition). The concentration of the lipid has been optimized just above the critical density for the lipid formation. If lower concentrations; around 0.2 mg ml^{-1}, were used, vesicles were observed at the surface but the density was not high enough to produce the bilayer and incomplete coverage was obtained.[28] The bilayer is stable over several days and the diffusion coefficient remains constant although fresh bilayers were prepared on a daily basis in all experiments described here.

The PEG 8000 solution at 30% wt/wt in aqueous buffer was introduced into the chamber by exchanging the contacting buffer with 2 ml of PEG 8000 solution. Then, after 5 min of incubation with the solution of PEG 8000, the solution in the chamber was again exchanged by flushing 10 ml of Tris buffer through the chamber. All prepared bilayers were replicated and studied a minimum of 5 times.

Instrumentation

All fluorescence measurements were carried out in the FCS2 closed chamber system, to control the temperature of the sample, and provide laminar flow in the chamber to promote efficient homogeneous exchange between the buffer and applied PEG solution. In addition the microscope objective was equipped with a heater to ensure there was no difference in temperature between the microscope objective and the bottom coverslip of the chamber. Both the chamber and the objective heater were purchased from Intracell (Royston, United Kingdom). The volume of the cell chamber was determined to be 347 ± 10 μl. A no. 1 coverslip was used for the bottom of the chamber and the coverslips were cleaned with ethanol following 20 min of plasma ozone treatment using a UV/Ozone Procleaner from bioforce (Ames, IA. US), before use.

Fluorescence lifetime correlation spectroscopy (FLCS)

The FLCS data were recorded using a Picoquant Microtime 200 system (Berlin, Germany). This set-up comprised an inverted XI 71 Olympus microscope, with a laser fiber optic coupling unit and dual SPD detection unit. A 60× NA 1.2 water immersion objective (UPlanSApo 60× 1.2 water/CC1.48, Olympus) was employed. Two pulsed picosecond lasers were used, a 532 nm laser PicoTA from Toptica (Picoquant) and 640 nm picosecond laser diode LDH-P-C-640B from Picoquant. A single mode optical fiber guides the two lasers to the main unit and provides a homogeneous Gaussian profile for the both excitations. The lasers are pulsed at 20 MHz, corresponding to an interval of 50 ns. Fluorescence was collected through the microscope objective and a dichroic mirror z532/635rpc blocked the backscattered light and HQ550lp AHF/Chroma for 532 nm and HQ670lp AHF/Chroma for 640 nm filters were used to clean up the signal. A 50 μm pinhole was used to confine the volume of detection in the axial direction. Fluorescence was detected using a SPAD from MPD (Picoquant). The time-correlated single photon counting system (PicoHarp 300 from Picoquant), that enabled simultaneous assessment of the lifetime in a nanosecond range along with the time of diffusion in the millisecond range.[29]

Data analysis

The autocorrelation function was constructed from fluorescence lifetime correlation spectroscopy data. The signal was filtered using time correlation single photon counting (TCSPC) to eliminate any contribution from after-pulsing[29,30] suppress scattered light and parasitic signals and most of the background.[31] The autocorrelation curves are fitted with a 2-dimensional model of diffusion, eqn (1), which takes into account the anomalous diffusion coefficient and in some cases the presence of 2 groups of molecules featuring different rates of diffusion:[9,32,33]

$$g^{(2)}(\tau) = \sum_i \frac{1}{N_i}\left(1 + \left(\frac{\tau}{\tau_{\mathrm{dif},i}}\right)^{\alpha_i}\right)^{-1} \quad (1)$$

where $g^{(2)}$ is the autocorrelation function, N is the average number of particles in the volume of excitation, τ_{dif} is the time of diffusion and α is the anomalous parameter which reflects the extent of deviation of diffusion from normal or Brownian motion where $\alpha = 1$ (ref. 34). i is the index of the components. The coefficient of diffusion D is obtained as $\tau_{\mathrm{dif}} = \omega^2/4D$, where ω is the length scale of the measurement, experimentally defined as the dimensions of the beam waist. To determine ω for each excitation, a reference solution of free dye was used for which the diffusion coefficient is known. For the excitation at 640 nm, the parent dye was Atto-655 in water at 25 °C and its coefficient of diffusion is 426 $\mu m^2\ s^{-1}$.[35] In the case of excitation at 532 nm, (used with the NapthBODIPY probe) a solution of rhodamine6G was used and it displays a diffusion coefficient at 300 $\mu m^2\ s^{-1}$ at 25 °C.[36] The fits of the autocorrelation curves are carried out using the Picoquant software package using a least squares

Marquard Levenbery algorithm. Goodness of fit was assessed on the basis of visual inspection of the residuals trace, and the χ^2 value. For an acceptable fit, no trend in the residuals trace should be observed, and χ^2 is found between 0.7 and 1.[37] (ESI†).

Results

The quality of the bilayers produced on ozone treated glass coverslips using the vesicle adsorption method, was assessed using confocal fluorescence imaging and FLCS measurements for bilayers in contact with Tris buffer solution. Following lipid bilayer assembly and assessment, a PEG 8000 solution was injected and incubated in the chamber following by extensive flush through with blank Tris buffer to remove PEG in the contacting solution, then the second set of measurements was recorded. The autocorrelation curves and their best fits according to eqn (1) are shown in Fig. 1–3. The fitted parameters, including D the coefficient of diffusion and α the anomalous parameter, are summarized in the Table 1.

The first lipid composition studied was 2-dioleoyl-*sn*-glycero-3-phosphocholine, DOPC. DOPC is a zwitterionic, unsaturated phospholipid widely used to create biomimetic cell membranes. The coefficient of diffusion of a planar supported bilayer of this lipid on plasma oxidized glass was obtained from FLCS using Atto-655–DOPE as reporter, as 7.9 $\mu m^2 s^{-1}$ ($\pm$0.2) with $\alpha = 1.02$ ($\pm$0.01). These values indicate a high lipid fluidity as the values are 2 to 3 times higher than typically reported for planar supported bilayers of DOPC on for example, glass or mica,[8] and are more consistent with those reported for diffusion observed for a GUV of this lipid rather than a planar layers.[38] This result suggests that ozone treatment of the glass substantially increases the fluidity of the contacting lipid layer. This was investigated using contact angle measurements. Significantly, measurements of water droplets on clean, untreated glass reveal a contact angle of approximately 50° while such droplets spread fully, *i.e.*, no measurable contact angle, is observed for the ozone treated surfaces. This indicated that ozone plasma treatment renders the glass superhydrophilic. The ability of ozone treated glass to disrupt lipid vesicles has been reported but this is the first report, to our knowledge, on the lipid dynamics on superhydrophilic glass using FLCS or FCS.[26] In contrast, when the coverslip is merely treated with a standard detergent such as Hellmanex, the diffusion coefficient was approximately 4–5 $\mu m^2 s^{-1}$, which is consistent with the reported literature on glass supported DOPC bilayers.[39,40]

To assess the impact of PEG exposure on the lipid diffusion properties, the bilayer was incubated for 5 min at 25 °C with a buffered aqueous solution containing 30% wt/wt PEG 8000 solution. This was introduced to the film and flushed from the chamber after incubation with 30 times the volume of the chamber with blank buffer (10 ml) to remove any weakly bound PEG from the surface. The autocorrelation curve was then recorded, and, as shown in Fig. 1(a), a substantial change in the profile was observed following PEG exposure. The membrane fluidity apparently increases and a diffusion coefficient of 51.4 $\pm$ 2.26 $\mu m^2 s^{-1}$, and α of 1.17 ($\pm$0.02) are observed. As α exceeds 1 it suggests anomalous diffusion is occurring.[34]

The second planar lipid bilayer studied comprised DOPC but this time with a 20% molar ratio, of 1,2-dioleoyl-*sn*-glycero-3-phospho-L-serine (DOPS). The DOPS is a negatively charge phospholipid. No differences were observed in the diffusion coefficient or in α on incorporation of DOPS into the lipid bilayer by comparison with DOPC alone (Fig. 1(a) and Table 1). However, the response of the lipid dynamics to PEG exposure was influenced by the presence of DOPS. Although, as for the DOPC layer, an increase of the diffusion rate is observed on exposure to PEG wherein the FLCS curves superimpose in the

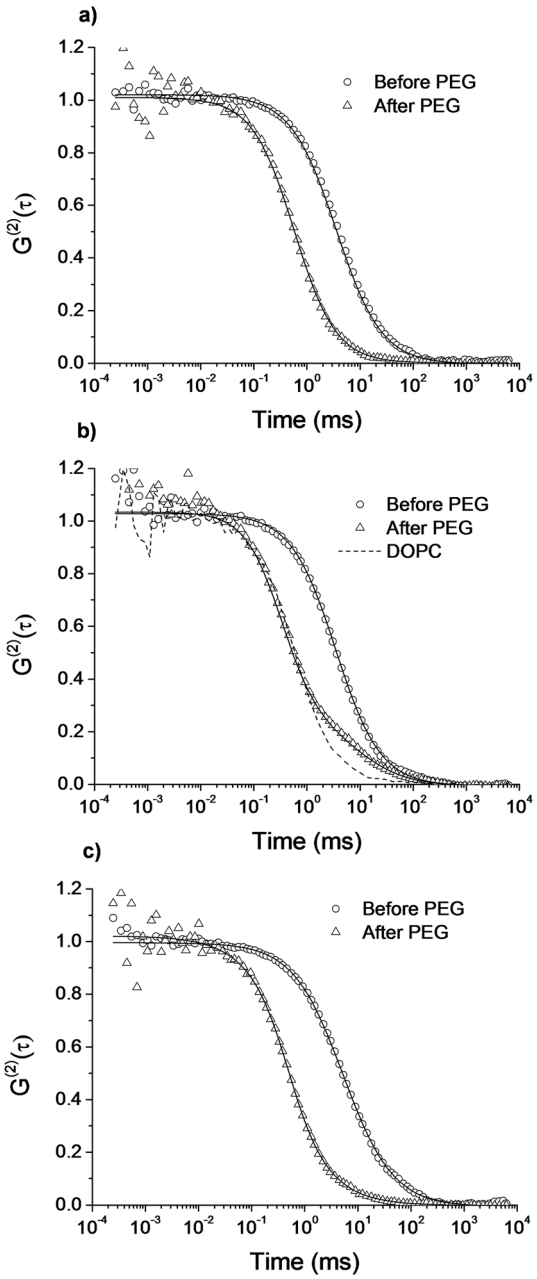

Fig. 1 Representative normalized FLCS autocorrelation curves for supported lipid bilayers on ozone plasma treated glass. The probe is the ATTO 655–DOPE excited at 640 nm Laser. (a) Represents pure DOPC, (b) DOPC/DOPS (80/20) and (c) pure DMPC. Circles (triangles) represent the curves recorded before PEG 8000 exposure, (respectively) after PEG 8000 exposure. The solid lines represents the fit used from the eqn (1). The dashed curve in (b) represents the DOPC after PEG 8000 exposure (triangles in (a)).

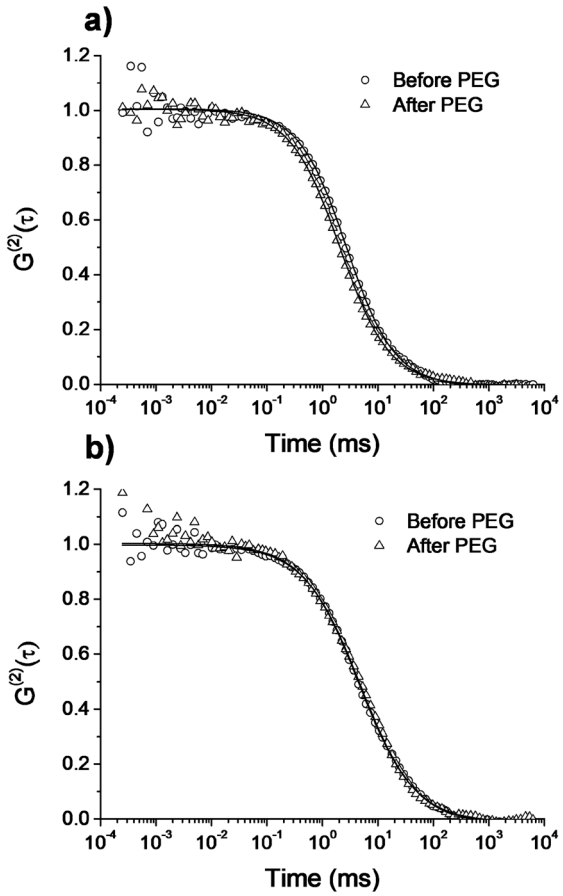

Fig. 2 Normalized autocorrelation curve from supported bilayer are calculated from the measurement acquired with 640 nm Laser. The probe observed here is the ATTO 655–DOPE. (a) Represents DOPC/Chol (60/40), (b) DOPC/DOPS/Chol (48/12/40). Circles (triangles) represent the curves recorded before PEG 8000 exposure, (respectively) after PEG 8000 exposure. The solid lines represents the fit using from the eqn (1).

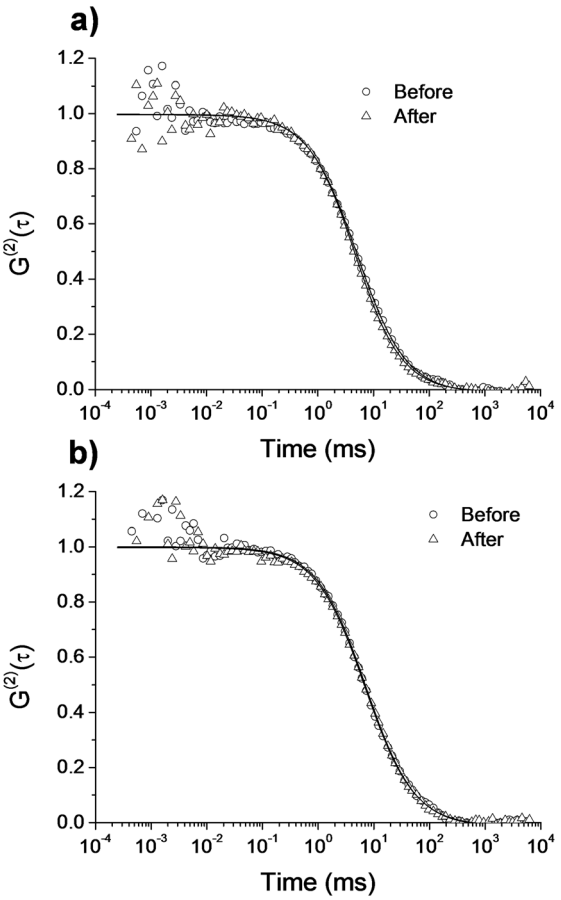

Fig. 3 Normalized autocorrelation curve of lipid bilayer containing NapthBodipy–DOPE as probe. The acquisition is recorded using the excitation at 532 nm. Circles and triangles represent the diffusion of the NapthBodipy probe in membrane before and after PEG 8000 exposure. The solid lines show the fit obtained with the eqn (1). (a) and (b) show respectively lipid mixture containing pure DOPC and DOPC/Chol (60/40).

short time domain, before 1 ms. In addition, an obvious deviation in the curves appeared for times longer than approximately 1 ms (Fig. 1(b)). The resulting shape of the autocorrelation curve required a two-component model for adequate fit, corresponding to eqn (1) with $i = 2$. The result of the fit shows a fast component with D_1 at 82 ± 5 μm^2 s^{-1} and α_1 at 1.28 ± 0.06 and a short component with D_2 at 2.8 ± 0.3 μm^2 s^{-1} and α_1 at 1.02 ± 0.07.

For planar bilayers of 1,2-dimyristoyl-*sn*-glycero-3-phosphocholine, DMPC, the hydrophilic functional group of this zwitterionic phospholipid is the same as PC, but the alkyl chain is saturated leading to an increased phase transition temperature for DMPC to approximately 23.5 °C. After formation of the fluid phase lipid bilayer on glass at 25 °C, the temperature was decreased to 22 °C to convert the bilayer from fluid phase to gel phase. Correspondingly no autocorrelation of the fluorescent signal was observed at the lower temperature, indicating the bilayer is immobile or that diffusion is very slow and the probe bleached. This result indicates that at 25 °C the system is very close to the phase transition for the DMPC bilayer.

Before PEG exposure, the diffusion coefficient is in the same range as observed for the other layers DOPC or DOPC/DOPS albeit slightly lower, 5.5 ± 0.1 μm^2 s^{-1}. However, α is below 1 with a value at 0.90 ± 0.01, this indicates sub-diffusion where the molecule's translational motion are hampered by obstacles, consistent with a temperature close to the gel phase temperature. Fig. 1(c), shows the autocorrelation data for the DMPC bilayer following exposure to PEG. A two component fit yielded a fast component with $D = 55 \pm 2.9$ μm^2 s^{-1}, $\alpha = 1.14 \pm 0.01$ and a slow component with $D = 4.8 \pm 1.8$ μm^2 s^{-1}, $\alpha = 0.74 \pm 0.02$.

A 40% molar ratio of cholesterol (Chol) was then introduced into the DOPC and DOPC/DOPS lipid film compositions during formation of their associated vesicles. Fig. 2(a), shows the fluorescence autocorrelation curves for Atto-655–DOPE probe at planar supported DOPC/Chol on plasma treated glass. Within experimental error, the films showed negligible change to diffusion coefficient, at 9.1 ± 2.3 μm^2 s^{-1} for the DOPC/Chol compared to the films without cholesterol, 7.9 ± 0.2 μm^2 s^{-1}. Following exposure to PEG, the autocorrelation curves still follow a one-component model which reveal a small increase in the coefficient of diffusion; from 9.1 ± 2.3 μm^2 s^{-1} to 11.9 ± 1.3 μm^2 s^{-1} with α of 0.98 ± 0.04 and 0.93 ± 0.03, respectively before and after PEG treatment of the DOPC/Chol film. In the case of DOPC/DOPS/Chol no increase is observed for the diffusion

Table 1 Summary of results from the fits applied using the eqn (1) corresponding to the solid line in Fig. 1–3. *i* is index the components, α is the anomalous parameter and *D* is the diffusion coefficient. "Atto 655" or "NapthBodipy" corresponding respectively to Atto-655–DOPE and Bodipy–DOPE indicates the probes used in each case. Results are shown for the experiment before and after PEG 8000 exposure

		Before PEG		After PEG	
Lipid composition	i (D_i α_i)	α	D (μm^2 s^{-1})	α	D (μm^2 s^{-1})
DOPC (Atto 655)	1	1.02 ± 0.01	7.9 ± 0.2	1.17 ± 0.02	51.4 ± 2.26
	2	—	—	—	—
DOPC/DOPS (Atto 655)	1	1.01 ± 0.02	7.9 ± 0.4	1.02 ± 0.07	2.87 ± 0.3
	2	—	—	1.28 ± 0.06	82 ± 5
DMPC (Atto 655)	1	0.9 ± 0.01	5.5 ± 0.1	1.03 ± 0.02	57.5 ± 3.41
	2	—	—	—	—
DMPC[a] (Atto 655)	1	—	—	0.74 ± 0.02	4.8 ± 1.8
	2	—	—	1.14 ± 0.01	55 ± 2.9
DOPC/Chol (Atto 655)	1	0.98 ± 0.04	9.1 ± 2.3	0.93 ± 0.03	11.97 ± 1.3
	2	—	—	—	—
DOPC/DOPS/Chol (Atto 655)	1	0.89 ± 0.03	6.62 ± 0.4	0.96 ± 0.12	9.3 ± 2.76
	2	—	—	1.53 ± 0.35	0.65 ± 1.1
DOPC (Bodipy)	1	0.98 ± 0.02	4.75 ± 0.1	1 ± 0.01	5.4 ± 0.3
	2	—	—	—	—
DOPC/Chol (Bodipy)	1	0.97 ± 0.02	3.33 ± 0.15	1.00 ± 0.01	3.4 ± 0.09
	2	—	—	—	—

[a] Represents the second fit applied to DMPC using a model with 2 components.

coefficient following PEG exposure. However, before PEG exposure the behavior is well described by the one component model using an α of 0.89, suggesting sub-diffusion behavior. In contrast, after PEG treatment, the fit using eqn (1) is less acceptable, the residual trace is less centered on zero, and the standard deviation is larger. The cholesterol introduction seems in this case to bring more disorder in the lipid organization and the fit is more approximate although the autocorrelation curves are similar to those seen in Fig. 2(b).

The incorporation of 40% (mole ratio) cholesterol into the DMPC bilayer immobilizes the film at 25 °C which is attributed to an increase in the phase transition temperature induced by the cholesterol. This was confirmed as diffusion was observed once the temperature was increased to approximately 30 °C. Further experiments were not pursued at this temperature as the PEG absorption is likely to be temperature dependent.

In order to gain insight into the role of the probe in accurately reporting the changes to the lipid diffusion, a series of experiments was conducted using a different dye while keeping the lipid tail constant. Using the NapthBodipy conjugated to DOPE (Scheme 1), we investigated the diffusion rates of this probe before and after PEG exposure to bilayers of pure DOPC and DOPC/Chol (60/40). Interestingly, in sharp contrast to the data reported above, the shapes of the curves are altered only very slightly by PEG treatment, and remain very close to those observed in the absence of PEG (Fig. 3) when NapthBodipy–DOPE was used as probe. The diffusion coefficients observed for the lipid bilayers prior to treatment with PEG are slightly lower than reported by the Atto-655 probe, $D = 4.8 \pm 0.1$ μm^2 s^{-1} for DOPC and the $D = 3.3 \pm 0.2$ μm^2 s^{-1} for DOPC/Chol. Most significantly, little change to the diffusion coefficient was observed after PEG treatment of the bilayer when NapthBodipy was used as a probe, 5.4 ± 0.03 μm^2 s^{-1}, for DOPC, 3.4 ± 0.09 μm^2 s^{-1}. Moreover the parameter α stayed very close to unity in all four cases (Table 1). The key difference between the two probes in the context of reporting on lipid bilayer behavior is that

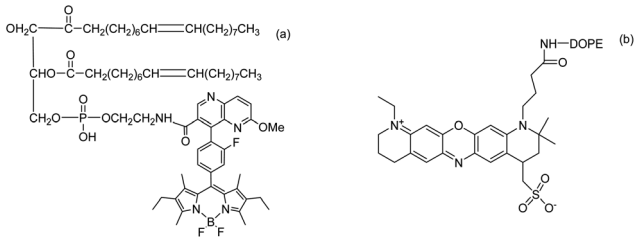

Scheme 1 Schematic of the molecular structure of (a) NapthBodipy DOPE conjugate and (b) Atto 655 DOPE conjugates. The structure of the lipid DOPE, 1,2-dioleoyl-*sn*-glycero-3-phosphoethanolamine, is shown in (a) but represented as DOPE in (b).

NapthBodipy is considerably more hydrophobic than the Atto 655, which, in contrast to the NapthBodipy is zwitterionic and soluble in water. As envisaged in Scheme 2, this is likely to result in partitioning of each probe into different regions of the bilayer, *i.e.*, in the case of the Atto 655, the probe will lie at the exterior interface of the lipid bilayer oriented toward the hydrophilic head groups and aqueous interface of the bilayer with shallower penetration of the probe and its tail into the lipid bilayer whereas NapthBODIPY, is likely to penetrate deeply into the hydrophobic interior of the layer away from the aqueous interface.

The luminescent lifetimes of the probes are expected to depend on the microenvironment of the dye and may therefore provide insight into the position of the probe in the bilayer. The emission lifetime of the dye was recorded during the FLCS measurement. The Atto-655 displayed no change in its emission lifetime of 2.8 ± 0.15 ns across the different lipid mixtures. However it's lifetime decreased to 2.3 ± 0.1 ns after PEG exposure. In the case of NapthBodipy, the lifetime observed was 6.0 ± 0.05 ns both with and without PEG treatment, but this value increase to 6.7 ± 0.06 ns in presence of cholesterol.

This suggests that the Atto-655 occupies a similar environment in all lipids in the absence of PEG, consistent with it orientation above the lipid aqueous interface but suggests an environmental

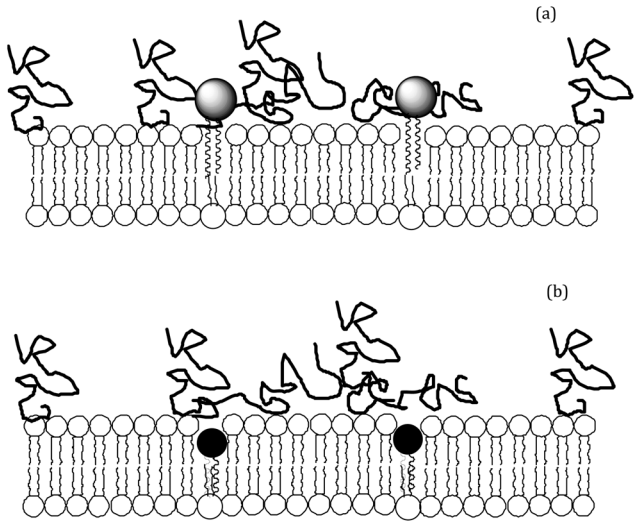

Scheme 2 Cartoon, not to scale, illustrating the explanation as to why the diffusion of the hydrophilic Atto-655–DOPE probe (a) and the hydrophobic Naphth-Bodipy–DOPE probes (b) are influenced to different extents on treatment of supported lipid bilayer with PEG. It is thought the affinity of the hydrophilic Atto-655 probe draws it closer to in the lipid–PEG interface in the layer where its diffusion is dictated by the PEG polymer meshes formed at the interface. Whereas the hydrophobic Naphth-Bodipy orients deeper within the lipid film away from the hydrophilic interface where it is uninfluenced by PEG, but where it reports more directly on the lipid diffusion.

change when PEG is present, indicating its partitioning into the hydrophilic PEG mesh when it is associated with the bilayer. The NapthBODIPY lifetime (and its diffusion rate) is unaffected by the presence of PEG, which would seem to confirm that it is located deeper within the bilayer. The cholesterol which is largely hydrophobic penetrates to the hydrophobic interior of the bilayer, thus affecting the NapthBODIPY environment and thus it's fluorescent lifetime. Again, this is consistent with penetration of the NapthBODIPY into the interior of the bilayer.

Discussion

PEG polymer is widely used for fusion of cells and vesicles and for lipid bilayer formation,[15,16,21] common protocols employ the addition of 30–40% (wt/wt) of PEG in aqueous media. Although many groups have discussed the influence of PEG on the fusogenic properties of PEG, there have been few reports on the effect of PEG on the fluidity of the lipid bilayer. Using ESR, Lee *et al.* proposed a model for the interaction between PEG molecules and lipid bilayer.[6] Their results suggested that PEG intercalates at the external aqueous interface of the lipid bilayer between the PC groups. Furthermore, interaction between the PEG molecule and PC head groups can then lead to a surface layer mesh of PEG at the hydrophilic interface of the membrane. The results presented here broadly support this picture.

The supported DOPC bilayer exhibits fast lateral lipid diffusion on the ozone plasma treated glass surface which conforms, on the basis of the fitted model, to free Brownian motion without any contribution from anomalous diffusion. After PEG exposure, the diffusion coefficient of the DOPE conjugated Atto within the lipid bilayer increased dramatically to 51.4 $\mu m^2 s^{-1}$ and α increased significantly to 1.17. α is a valuable measure of the nature of the 2D diffusion.[9] An α of 1 indicates free Brownian diffusion, α below 1 is referred to as sub-diffusion and is taken to indicate the motion of the molecule is hampered by a mobile or immobile obstacle, for example by the presence of a microdomain. For α above 1, the diffusion is described as super-diffusion[10,34] and has been suggested to be due to the directional diffusion of molecules confined to travel along restricted 2-dimensional pathways .[41] Angelico *et al.*[23] studied the anomalous diffusion of a surfactant in a "living polymer system" involving a mixture of lecithin worm-like micelles. They described this type of diffusion in terms of a fractal model with a free particle travelling along network meshes and predicted an enhancement of the diffusion if the fractal dimension is less than 2. The FLCS data presented here is consistent with such a model. We speculate that if the PEG polymer forms discontinuous hydrophilic mesh domain on the 2-dimensional lipid bilayer surface, it could create a favorable path along which the hydrophilic part of the bilayer DOPE–Atto 655 probe can diffuse. These paths form as defects presenting a ripple phase that allows a faster diffusion.[34] Moreover, the hydrophilic character of the Atto-655, which is water soluble in its basic form, would be expected to have strong affinity with such a PEG mesh. Consistent with its partitioning into such meshes, the fluorescence lifetime of the Atto-655 exhibits a small but significant decrease from 2.8 ± 0.15 to 2.3 ± 0.1 ns when the lipid layer is exposed to PEG.

To assess if the Atto-655–DOPE diffusion truly reflects the diffusion of the lipid bilayer or reflects diffusion of this probe through such interfacial mesh domains we assessed the diffusional behavior of a hydrophobic probe, NapthBodipy, under the same conditions. The NapthBodipy–DOPE probe, Scheme 1 is hydrophobic and completely water insoluble. Therefore expected to penetrate relatively deeply into the lipid bilayer away from the aqueous/PEG interface. These experiments reveal that in sharp contrast to the Atto dye, the NapthBodipy labeled lipid diffusion was completely insensitive to PEG exposure of the lipid film. This contrasting behavior between the hydrophobic and hydrophilic probes provides convincing evidence that rather than a change in the overall fluidity of the membrane, the PEG forms fluid domains or paths along which the hydrophilic probe is transported.

Similar results are observed with a planar DMPC bilayer wherein an increase in the diffusion coefficient was observed for the Atto-655 probe on exposure of the film to PEG. However, the transition temperature is around 23.5 °C for DMPG in contrast to just 2 °C for DOPC. Therefore, for DMPC, the experimental temperature is close to the gel–fluid transition, so that before PEG treatment, α is 0.9 corresponding to sub-diffusion. Favard *et al.*[34] observed that when the temperature is close to the transition of DMPC (even slightly above), the FCS diffusion laws exhibit anomalous behavior, *i.e.* deviating from pure Brownian motion as the lipid bilayer is not in a purely fluid state. We observed that when PEG was introduced, the coefficient of diffusion increased from 5.5 to 57.5 $\mu m^2 s^{-1}$ whereas α increased to 1.02, corresponding apparently to free Brownian diffusion. Surprisingly, this is somewhat at odds with previous observations of α on the same lipid composition, *i.e.* pure DMPC. Nevertheless, Angelico *et al.* explained that an apparent normal diffusion regime can be due to a transition state between super

and sub-diffusion behavior. Those studies were conducted using NMR, but NMR and FCS results can be compared as the temporal range accessible for diffusion of lipid with both methods are in the same range (1–10 $\mu m^2 s^{-1}$).[42,43] Correspondingly, when a two-component model was used to model the data a satisfactory fit was achieved. It should be noted that in the present case, the fit either with one or two-components models leads to a very similar quality of fit under the criteria of the residual trace (ESI†). We obtained a fast component ($D = 55 \pm 2.9\ \mu m^2 s^{-1}$) with $\alpha = 1.14 \pm 0.01$ and a slow component ($D = 4.8 \pm 1.8\ \mu m s^{-1}$) with $\alpha = 0.74$ attributed respectively to a fast super-diffusion and a slow sub-diffusion.

The introduction of DOPS, a negatively charge lipid, into the DOPC bilayer did not change the diffusion rate or cause it to deviate from Brownian motion. However, after PEG introduction, the FCS curves change significantly compared with PEG treated DOPC alone. The curve no longer conformed to a single component model but required a two-component model for an adequate fit and features a fast component with $\alpha = 1.28$ and slower component with $\alpha = 1.02$. These values indicate the presence of regions of normal diffusion and super-diffusion. Again, this is suggestive of PEG mesh formation. That both a fast and slow component are observed here, but not in the DOPC only film, suggests that the probe partitions into the PEG domains in the DOPC film but is distributed in both environments in the DOPC/DOPS film, which may be due to the negative charge on the DOPS lipid. The Atto-655 probe is zwitterionic and the positively charged group on the probe may associate more strongly with the DOPS. In addition, the tendency of DOPS to form domains has been reported in the past. For example, using AFM, Brisson *et al.* observed clear changes in the morphology of the DOPS containing bilayer into nanoscopic domains when the membrane is surrounded by a solvent containing Ca^{2+}.[11]

Finally, the effect of the presence of cholesterol in the lipid film on the influence of PEG was examined. As shown in Fig. 2, in stark contrast to behavior in the absence of cholesterol, for the DOPC/Chol bilayer no increase in fluidity of the film was evident when PEG is added. Although the fluidity of the bilayer is comparable with and without cholesterol, the organization of the lipid bilayer is expected to change. Indeed the cholesterol is known to decrease the difference between liquid and gel phase in a heterogenic mixture, creating an intermediate state.[44]

In contrast, when cholesterol is added to DOPC/DOPS, the diffusion coefficient decreases by a small but significant degree and α is determined to be 0.89. The cholesterol is more likely to modify the ordering of the lipid in the membrane DOPC/DOPS heterogeneously, which could be attributed to the higher affinity of cholesterol for PC than for PS.[44] Therefore, the formation of domains in the mixture may be responsible for the observation of non-Brownian sub diffusion displaying $\alpha < 1$.

The key result is that when cholesterol is introduced the PEG does not appear to exert the same influence on the membrane with no evidence for super-diffusion of the Atto probe on PEG exposure when cholesterol is present. The cholesterol is known to introduce conformational ordering in the lipid chains which has an effect on the stiffness and thickness of the membrane. This is thought to decrease the cross sectional area of the phospholipids and increase the orientational order.[44] The results reported here suggest that intercalation of the PEG at the hydrophilic head groups of the lipid is compromised by the presence of cholesterol. However, that the data does not fit well to the conventional 1 or 2 component model suggests the behavior is complex and confirms that the PEG does perturb the lipid dynamics in the presence of cholesterol.

The NapthBodipy probe exhibits little sensitivity to the presence of cholesterol in terms of its diffusion, although its fluorescence lifetime is affected. The NapthBodipy probe, in absence of cholesterol exhibits no change in lifetime after film PEG exposure, the fluorescence lifetime was 6.0 ± 0.05 ns in both cases. However, when cholesterol is introduced into the lipid mixture, we observe a small increase to 6.7 ± 0.06 ns and then no further change in lifetime when this film was treated with PEG. Consistent with the lifetime data, these studies indicate that the NapthBodipy tends to penetrate more into the hydrophobic interior of bilayer where it is not affected by the PEG but where it does experience changes to its environment caused by cholesterol which will similarly penetrate to the hydrophobic interior. As such this probe may more accurately reflect the fluidity of the lipid bilayer.

Conclusions

Fluorescence lifetime correlation spectroscopy (FLCS) was employed to assess the impact of PEG-8000 polymer treatment of planar suspended lipid bilayer on the fluidity of the bilayer. The effect of PEG as a function of lipid composition, the presence of cholesterol and hydrophilicity of fluorescent probe was explored. The lipid bilayers explored were assembled on ozone plasma treated glass. These superhydrophilic substrates were used to disrupt liposomes of different compositions to reproducibly yield defect-free bilayers which exhibited fluidity 2 to 3 times higher than typical for conventional glass or mica.

The analysis of FLCS data showed that using Atto 655 labeled DOPE as a probe, after adsorption of the PEG on the lipid bilayer surface, the rate of diffusion of the probe increased by nearly an order of magnitude. Depending on the lipid composition, bimodal diffusion was observed showing both a fast diffusive component and a slower component, more reminiscent of the bilayer before PEG treatment. Significantly, the mode of diffusion diverges from pure Brownian motion after PEG treatment with α for the fast component of the diffusion exceeding 1, which reflects super-diffusion. The addition of 40 mol% cholesterol to the bilayer modifies this behavior whereby PEG treatment does not appear to induce superdiffusion.

Strikingly, the observed behavior depends intrinsically on the nature of the probe. When using a hydrophobic probe conjugated to DOPE there was no evidence for anomalous diffusion when the lipid bilayers were treated by PEG. Indeed, the changes to the fluidity of the bilayers as reported by this probe were relatively minor. This difference in fluidity reported by the each probe is attributed to partitioning of the probes into different regions of the bilayer. These results suggest that PEG forms a surface layer mesh at the lipid bilayer surface leading to the creation of hydrophilic microdomains with which the Atto-655–DOPE preferentially associates. The faster diffusion of the Atto-655 probe along the mesh is associated with a particular mode of diffusion in fractal dimension ($D < 2$) called superdiffusion.

Because of the hydrophobic character of the NapthBODIPY, it lies deeper within the bilayer reporting from within the hydrophobic region of the bilayer whose fluidity is actually relatively unaffected by PEG as it adsorbs at the bilayer surface. The partitioning of the different probes into different domains is corroborated by changes to the lifetime of each probes as either PEG or cholesterol is added to the bilayer film.

Acknowledgements

This material is based upon work supported by the Science Foundation Ireland under Grant no. [10/IN.1/B3025] and the National Biophotonics and Imaging Platform, Ireland, funded by the Irish Government's Programme for Research in Third Level Institutions, Cycle 4, Ireland's EU Structural Funds Programmes 2007–2013. T.T. and TEK acknowledge support from NBIPI Career Enhancement and Mobility Fellowship co-funded by Marie Curie Actions.

References

1 D. M. Owen, D. Williamson, C. Rentero and K. Gaus, *Traffic*, 2009, **10**, 962–971.
2 M. J. Wilson, *J. Am. Chem. Soc.*, 1996, **118**, 6580–6587.
3 S. J. Singer and G. L. Nicolson, *Science*, 1972, **175**, 720–731.
4 L. Vigh, P. V. Escribá, A. Sonnleitner, M. Sonnleitner, S. Piotto, B. Maresca, I. Horváth and J. L. Harwood, *Prog. Lipid Res.*, 2005, **44**, 303–344.
5 E. I. Goksu, J. M. Vanegas, C. D. Blanchette, W.-C. Lin and M. L. Longo, *Biochim. Biophys. Acta*, 2009, **1788**, 254–266.
6 D. K. Lee, J. S. Kim, Y. M. Lee, Y. S. Kang and B. K. Kim, *Langmuir*, 1998, **14**, 5184–5187.
7 S. Chiantia, J. Ries and P. Schwille, *Biochim. Biophys. Acta*, 2009, **1788**, 225–233.
8 R. Machán and M. Hof, *Biochim. Biophys. Acta*, 2010, **1798**, 1377.
9 L. Wawrezinieck, H. Rigneault, D. Marguet and P.-F. Lenne, *Biophys. J.*, 2005, **89**, 4029.
10 D. J. Verkman, *Annu. Rev. Biophys.*, 2008, **37**, 247.
11 I. Reviakine, A. Simon and A. Brisson, *Langmuir*, 2000, **16**, 1473.
12 R. Böckmann, A. Hac, T. Heimburg and H. Grubmüller, *Biophys. J.*, 2003, **85**, 1647.
13 T. Auth, S. Safran and N. S. Gov, *New J. Phys.*, 2007, **9**, 430.
14 M. Barz, R. Luxenhofer, R. Zentel and M. J. Vincent, *Polym. Chem.*, 2011, **2**, 1900.
15 M. E. Haque, T. J. McIntosh and B. R. Lentz, *Biochemistry*, 2001, **40**, 4340.
16 W. Guo, J. Peter and T. K. Vanderlick, *Ind. Eng. Chem. Res.*, 2006, **45**, 5512.
17 A. Martin, C. Long, R. J. Forster and T. E. Keyes, *Chem. Commun.*, 2012DOI: 10.1039/C2CC31150J.
18 K. R. Poudel, D. J. Keller and J. Brozik, *Langmuir*, 2011, **27**, 320.
19 A. J. Diaz, F. Albertorio, S. Daniel and P. S. Cremer, *Langmuir*, 2008, **24**, 6820.
20 M. Tanaka and E. Sackmann, *Nature*, 2005, **437**, 656.
21 A. Berquand, P. E. Mazeran, J. Pantigny, V. Proux-Delrouyre, J. M. Laval and C. Bourdillon, *Langmuir*, 2003, **19**, 1700.
22 T. Kuhl, Y. Guo, J. L. Alderfer, A. D. Berman, D. Leckband, J. Israelachvili and S. W. Hui, *Langmuir*, 1996, **12**, 3003.
23 R. Angelico, A. Ceglie, U. Olsson, G. Palazzo and L. Ambrosone, *Phys. Rev. E: Stat., Nonlinear, Soft Matter Phys.*, 2006, **74**, 031403.
24 T. Dertinger, I. von der Hocht, A. Benda, M. Hof and J. Enderlein, *Langmuir*, 2006, **22**, 9339.
25 E. Kalb, S. Frey and L. K. Tamm, *Biochim. Biophys. Acta*, 1992, **1103**, 307.
26 R. Richter, A. Mukhopadhyay and A. Brisson, *Biophys. J.*, 2003, **85**, 3035.
27 I. Reviakine and A. Brisson, *Langmuir*, 2000, **16**, 1806.
28 See ESI†
29 M. Böhmer, M. Wahl, H.-J. Rahn, R. Erdmann and J. Enderlein, *Chem. Phys. Lett.*, 2002, **353**, 439.
30 J. Enderlein and I. Gregor, *Rev. Sci. Instrum.*, 2005, **76**, 033102.
31 P. Kapusta, M. Wahl, A. Benda, M. Hof and J. Enderlein, *J. Fluoresc.*, 2007, **17**, 43.
32 K. Vats, M. Kyoung and E. D. Sheets, *Biochim. Biophys. Acta*, 2008, **1778**, 2461.
33 K. Vats, K. Knutson, A. Hinderliter and E. D. Sheets, *ACS Chem. Biol.*, 2010, **5**, 393.
34 C. Favard, J. Wenger, P.-F. Lenne and H. Rigneault, *Biophys. J.*, 2011, **100**, 1242.
35 T. Dertinger, V. Pacheco, I. von der Hocht, R. Hartmann, I. Gregor and J. Enderlein, *ChemPhysChem*, 2007, **8**, 433.
36 C. B. Müller, A. Loman, V. Pacheco, F. Koberling, D. Willbold, W. Richtering and J. Enderlein, *EPL*, 2008, **83**, 46001.
37 U. Meseth, T. Wohland, R. Rigler and H. Vogel, *Biophys. J.*, 1999, **76**, 1619.
38 M. Przybylo, J. Sýkora, J. Humpolíckova, A. Benda, A. Zan and M. Hof, *Langmuir*, 2006, **22**, 9096.
39 A. Benda and V. Marecek, *Langmuir*, 2003, **9**, 4120.
40 M. Stefl, A. Kułakowska and M. Hof, *Biophys. J.*, 2009, **97**, L01.
41 L. Guo, P. Chowdhury, J. Fang and F. Gai, *J. Phys. Chem. B*, 2007, **111**, 14244.
42 P.-O. Gendron, F. Avaltroni and K. J. Wilkinson, *J. Fluoresc.*, 2008, **18**, 1093.
43 G. P. Holland, S. K. McIntyre and T. M. Alam, *Biophys. J.*, 2006, **90**, 4248.
44 T. P. W. McMullen, R. N. A. H. Lewis and R. N. McElhaney, *Curr. Opin. Colloid Interface Sci.*, 2004, **8**, 459.